Characterisation of nanoparticles by means of high-resolution SEM/EDS in transmission mode

2016 IOP Conf. Ser.: Mater. Sci. Eng. 109 012006

(http://iopscience.iop.org/1757-899X/109/1/012006)

IOP Conf. Series: Materials Science and Engineering **109** (2016) 012006 doi:10.1088/1757-899X/109/1/012006

Characterisation of nanoparticles by means of high-resolution SEM/EDS in transmission mode

V-D Hodoroaba[1], S Rades[1], T Salge[2], J Mielke[1], E Ortel[1] and R Schmidt[3]

[1] BAM – Federal Institute for Materials Research and Testing, Unter den Eichen 87, 12205 Berlin, Germany
[2] Natural History Museum, Core Research Laboratories, Cromwell Road, London SW7 5BD, Great Britain
[3] Hitachi High-Technologies Europe, Europark Fichtenhain 12A, 47807 Krefeld, Germany

E-mail: dan.hodoroaba@bam.de

Abstract. Advances in scanning electron microscopy (SEM) enable the high-resolution imaging of single nanoparticles (NPs) with sizes well below 10 nm. The SEM analysis in transmission mode (T-SEM) of NPs on thin film supports has many benefits when compared to the analysis of NPs on bulk substrates. The enhanced material (mass – thickness) contrast of the T-SEM imaging mode is well suited for in-depth and, particularly valuable, to very accurate, traceable, lateral dimensional measurements of NPs. Compared to samples prepared on bulk substrates, T-SEM with energy dispersive X-ray spectroscopy (EDS) achieves a drastically improved spatial resolution of the emitted X-rays. The poor signal-to-noise ratio of the X-ray spectra emitted by a single nanoparticle (NP) can be improved by the use of high-sensitivity (high collection solid angle) silicon drift (SDD), energy-dispersive X-ray spectrometers (EDS). The EDS spectral imaging of a single NP with a spatial resolution below 10 nm has become possible. This is demonstrated by means of various examples of nanostructures. Advanced data processing of T-SEM/EDS results sets the stage for the automated classification of NPs by feature analysis. This method combines the detection of morphological structures of interest by image processing of T-SEM micrographs with the chemical classification by EDS.

1. Introduction

Due to the application of nanoparticles (NPs) within commercial products, there is an increasing demand for SEM/EDS laboratories to characterise nanoparticulate materials. Technological improvements in SEM and within energy-dispersive X-ray spectrometry (EDS) allow the analysis of sample surface morphology, the inner structure and the elemental composition with a comparable spatial resolution in the nanometre range.

The conventional Everhart–Thornley (E-T) and the *In-Lens* detector of modern SEMs are able to image sample surface morphology at high spatial resolution to a sub-nm scale. In addition, STEM (scanning transmission electron microscopy) detectors collect transmitted electrons resulting in imaged NPs with a superior material (mass and thickness) contrast. For the latter option, the specimen must be prepared on an electron transparent thin supporting film which is analogue to the preparation for transmission electron microscopy (TEM).

Imaging by means of transmitted electrons in an SEM exploits the high signal-to-noise ratio resulting from the dominant "forward" electron scattering within a nanoscale sample. In addition, the transmitted electrons suffer reduced scattering events within the thin sample, resulting in an intense electron signal in transmission mode. Surface effects, such as charging and contamination are not as critical in comparison with the secondary electron (SE) imaging mode [1]. Hence, the SEM in transmission mode (T-SEM) provides a metrological tool for dimensional (lateral) measurements of NPs, i.e., particle size distribution [1-4], but is also well suited for "in-depth" observation of structured NPs [4, 5].

The direct measurement of nanoparticle (NP) size and shape/morphology by high-resolution, electron-beam based imaging techniques can be complemented by spatially resolved chemical information as offered by EDS. Two main technological developments have enabled the improvement of the spatial resolution of EDS analysis from micro- to nano-range: (i) The development of high-sensitivity, high solid angle SDD detectors, and (ii) the application of T-SEM by preparing the NPs on standard TEM grids. Hence, the weak X-ray signal emitted by a single NP on an electron-transparent supporting film can be detected with sufficiently high signal-to-noise ratio. The excited sample volume is drastically reduced in comparison to a bulk support.

Furthermore, it has recently been demonstrated that the "bulk" EDS analysis of NPs can be supplemented by chemical imaging of ultra-thin (up to a few nm) outer shells by scanning Auger electron microscopy (SAM) [6, 7]. The lateral resolution attained by this technique is in the order of 10 nm.

2. Experimental methods

In order to achieve high-resolution imaging from the upper-most surface of a specimen using an SEM, advanced detectors are required. These are used to selectively detect so-called SE1 electrons that are emitted locally at the point of interaction between the primary electron beam and the specimen surface. In this study the detector employed was an *In-Lens* SE detector (Zeiss Supra 40, FE-SEM, Oberkochen, Germany), see figure 1a. Additional selected images for studying the inner structure of silica particles have been included, that were obtained using a FE-SEM (Hitachi SU 8230, Tokyo, Japan) equipped with different electron detectors, see later figure 6.

The proof-of-principle of T-SEM was demonstrated over thirty years ago [8-10]. The application to the characterisation of NPs however, has only recently been reported [1-5, 11]. In particular, the capability of T-SEM to the metrological measurement of lateral dimensions in the nanometre range, e.g., for the purpose of accurate NP size and distribution determination, has already been successfully exploited. Basically, the STEM detector which is placed directly under the thin specimen (figure 1b) can be used for acquiring images in transmission mode in an SEM [12].

In this study, a commercially available transmission unit has been employed [13]. This consists of a specimen holder that guides the transmitted electrons (TE) onto an electron multiplier in the form of a gold plate located below the bright-field (or alternatively dark-field) aperture (figures 1c and 1d). The multiplied transmitted electrons are then collected by the conventional E-T detector. The screening ring (see figure 1d) prevents surface sample generated SE and BSE electrons from directly entering the E-T detector. On the other side, the screening ring in operation mode prevents also the X-rays emitted by the sample to reach the EDS detector, so that it is necessary to remove manually the ring before an EDS analysis. Furthermore, the single-unit transmission setup is designed for only one TEM grid. The TSEM detector can analyse up to four grids mounted in commercial sample holders and EDS can be carried out without being necessary to (re)move parts. Contrary to the STEM detector the single-unit setup works reliably at low energies (below 7 keV). Not unimportant, the single-unit transmission sample holder can be easily taken and inserted in any other SEM having a sample stage with dove-tail mount. Summing up, T-SEM imaging with the single-unit setup can be carried out practically with similar performance when compared to imaging using a STEM detector [1-4].

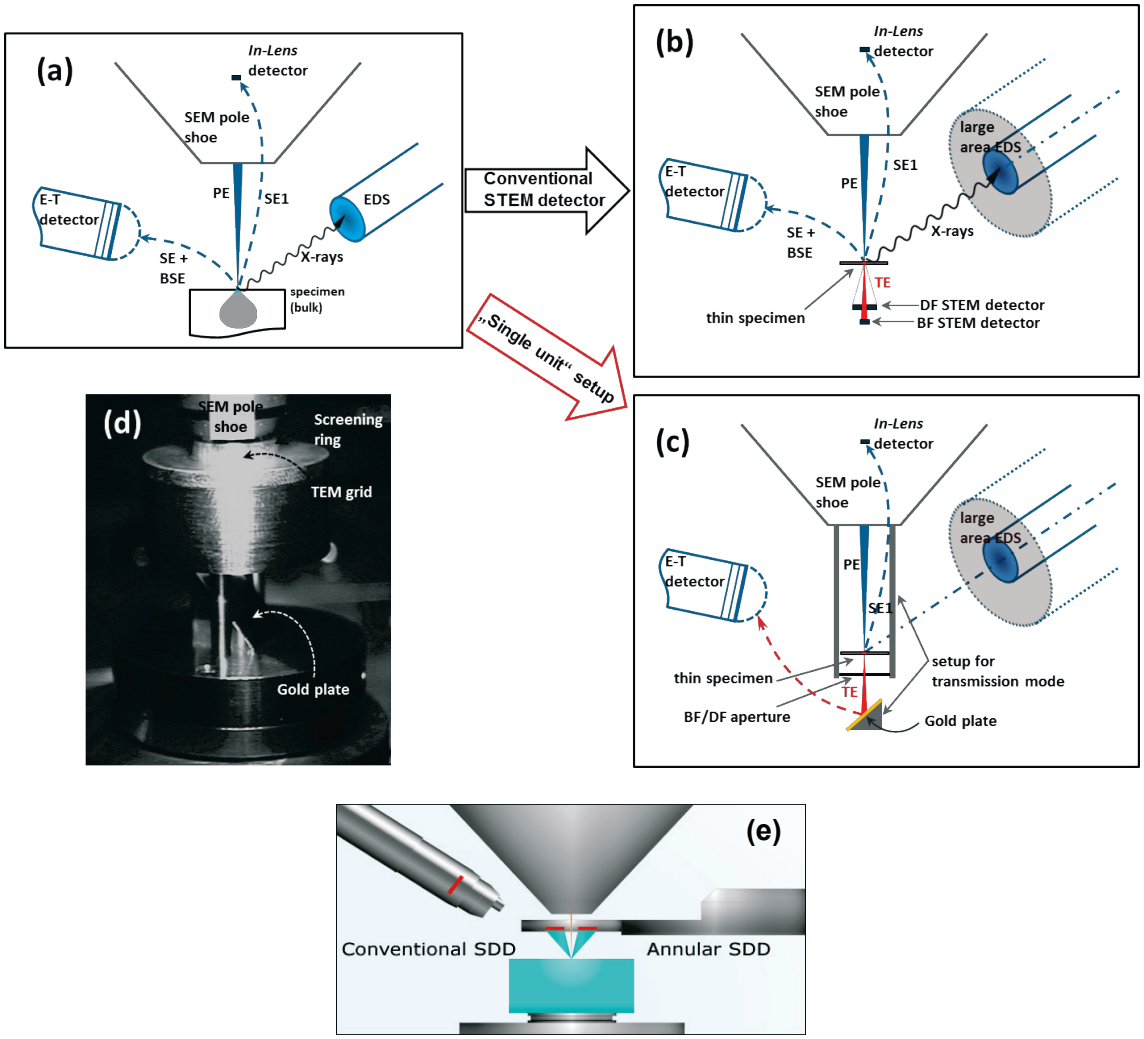

Figure 1. Schemes of various SEM/EDS configurations suited to various types of analysis: (a) Bulk sample analysis in a SEM showing a conventional E-T detector for the collection of SE/BSE electrons. SE electrons can also be collected with a high-resolution *In-Lens* SE detector. Note the relative large emission volume of X-rays which can be collected by an EDS detector. (b) Thin sample analysis: in addition to (a), the STEM detector collects only the transmitted electrons (operating either in bright or dark field mode). A larger active EDS detector area increases the collection efficiency of emitted X-rays. (c) Thin sample analysis in transmission mode (T-SEM) with the single-unit setup as used in this study. (d) Photograph of the T-SEM setup in working position (close to pole shoe). (e) Geometry of the annular SDD EDS encompassing a significantly larger solid angle (up to about 1 sr) compared to conventional SDD EDS.

In this study the following EDS detectors were used: a 10 mm^2 Si(Li) (Thermo Scientific, USA), a 10 mm^2 SDD (Bruker, Germany), a 100 mm^2 SDD (Thermo Scientific, USA), and an annular 60 mm^2 FlatQUAD SDD (Bruker, Germany). The annular SDD is inserted between the pole shoe and the sample, so that a very large solid angle of about 1 sr of the X-rays emitted by the sample can be encompassed (figure 1e). The corresponding collection solid angles of the 10 mm^2 and 100 mm^2 detectors amounted to about 6-7 msr and about 50 msr, respectively. Four detection segments of

15 mm^2 each around the central orifice for the primary electrons contribute to the total signal after parallel processing. For the classification of NPs, the automated feature analysis software of the Bruker Quantax EDS system was used with a 10 mm^2 SDD and an annular SDD, respectively.

3. Results and discussion

In order to test the analytical capabilities of high-resolution T-SEM/EDS, various materials containing NPs of known size (distribution) and chemical composition have been analysed. The first example focusses on particle size distribution (PSD) measurements of bimodal SiO_2 NPs which were prepared on carbon/*Formvar* TEM grids by aerosolisation (figure 2a). The superior material (mass- thickness) contrast of T-SEM imaging well suited to dimensional measurements can be observed in figure 2b. In addition, it reveals the presence of SiO_2 NPs also on the rear side of the thin foil (see the arrows in figure 2b and compare to figure 2a). For PSD measurements, binarisation of T-SEM micrographs, automatic counting and data reduction were performed using an open source image processing software, e.g., *ImageJ* [14]. The particles size evaluated as the PSD of the minimum Feret diameter extracted from the T-SEM micrographs as in figure 2b is presented in figure 2c. The validity of the T-SEM results has been demonstrated elsewhere by the good agreement with results obtained by TEM, SMPS and AFM analysis of the same material [3].

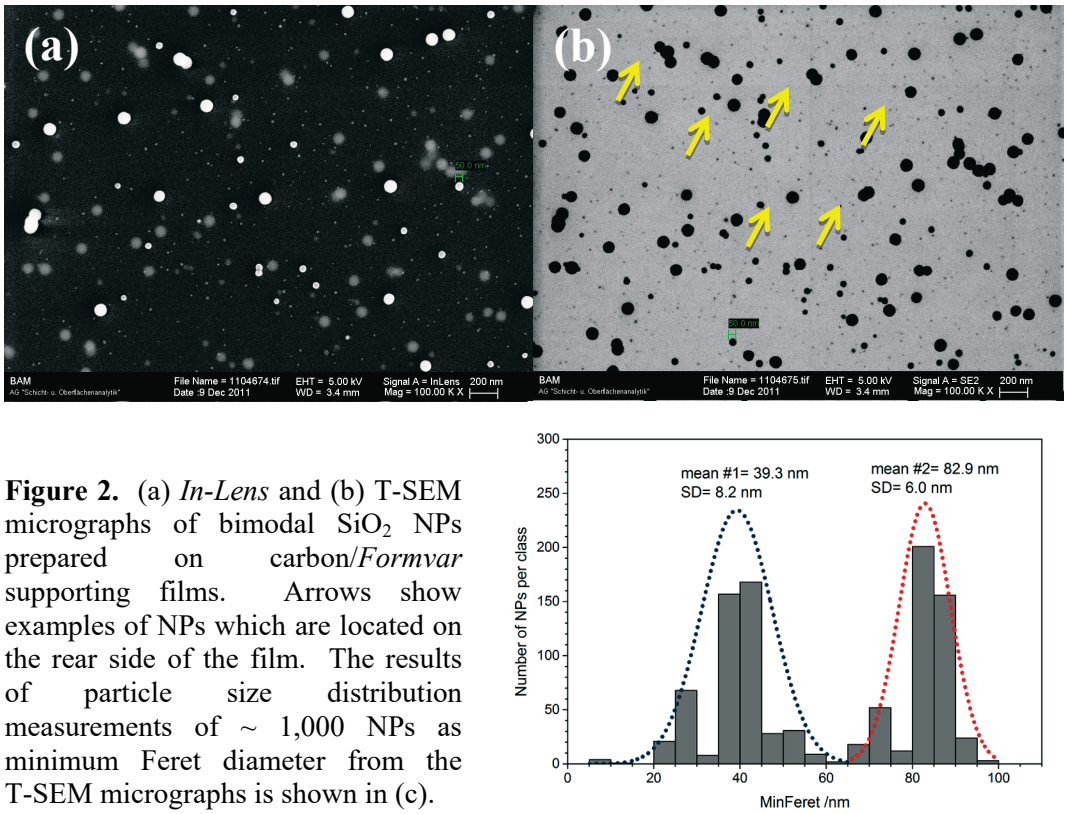

Figure 2. (a) *In-Lens* and (b) T-SEM micrographs of bimodal SiO_2 NPs prepared on carbon/*Formvar* supporting films. Arrows show examples of NPs which are located on the rear side of the film. The results of particle size distribution measurements of ~ 1,000 NPs as minimum Feret diameter from the T-SEM micrographs is shown in (c).

The second analysed sample represents a mixture of SiO_2 and TiO_2 NPs (figure 3). Imaging with a conventional E-T detector or even with an *In-Lens* detector may indicate the presence of two different NP types (see figure 3a). The high surface sensitivity of the *In-Lens* imaging only suggests the presence of some larger NPs between a rather monodisperse, smaller NPs. The evidence that there are two distinct NP types of different mid-atomic numbers, sizes (about 20 nm and 40 nm, respectively) and shapes is shown by the superior transmission imaging (mass-thickness) contrast of T-SEM

(figure 3b). It should be noted that the very good transmission contrast between the two types of NPs is enhanced additionally by the somewhat larger NPs of the heavier type.

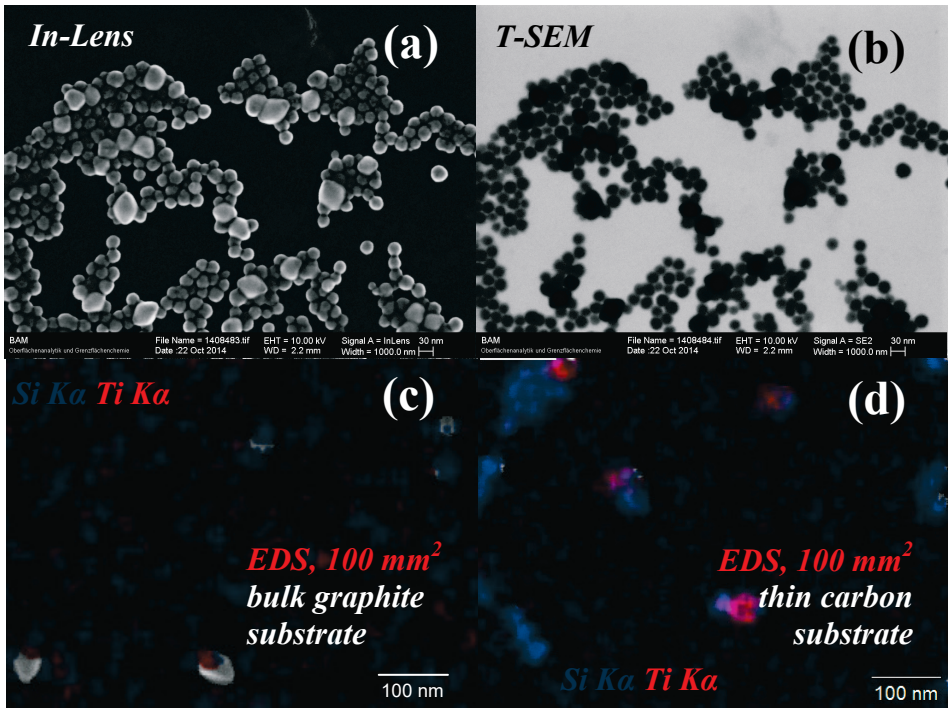

Figure 3. 10 kV imaging of a mixture of SiO_2 and TiO_2 NPs prepared on a thin, electron transparent, carbon foil TEM grid: (a) SE *In-Lens* mode (surface sensitive). (b) T-SEM mode (Z and thickness sensitive). (c) 10 kV EDS mapping overlain with SEM micrograph of the sample on a graphite bulk substrate (100 mm^2 SDD). (d) 10 kV EDS mapping overlain with SEM micrograph of the sample on a carbon foil TEM grid (100 mm^2 SDD). EDS data were enhanced with a map filter to reduce the local image noise situation.

To compare the benefit of T-SEM/EDS with conventional bulk EDS in respect to NPs elemental analysis, the material was prepared on a bulk graphite substrate and also on a thin carbon film. Figure 3c shows that on a bulk substrate, it is not possible to analyse the element distribution (figure 3c) due to the large contribution of the carbon substrate, even when a large-area, 100 mm^2 SDD is used. The discrimination between different NP types can be attained when the T-SEM/EDS approach is exploited (figure 3d).

The third example of a nanoparticulate material consists of gold NPs with an average particle size (diameter) of 17 nm. A 3 µL droplet of the initial Au suspension has been prepared on thin (lacey) carbon supporting foil (TEM grid). The T-SEM micrograph (figure 4a) shows that NPs are well dispersed on the carbon foil. The main interest of the analysis of this material was to compare the detection sensitivity of EDS detectors with various collection solid angles: (i) a conventional SDD with 10 mm^2 detector area, (ii) a new generation SDD with 100 mm^2 detector area, and (iii) and a state-of-the-art annular 60 mm^2 SDD detector. The 10 mm^2 SDD detector was not able to detect single Au NPs even after several minutes of acquisition. Longer acquisition times could not be considered due to significant image drifts. The elemental identification of the nanoparticulate material became possible by spectrum acquisition only from agglomerates (figure 4b). The 100 mm^2 SDD

(figure 4c) could provide the element distribution using the Au M X-ray line after about two minutes. With the annular SDD, the acquisition time for a similar map area could be significantly reduced to only 13 seconds (figure 4d). These results prove the capability of the annular EDS detector for rapid identification of the Au NPs with sizes below 20 nm. For NP materials with a low mean atomic number, such as oxides and polymers, the detection sensitivity decreases, so that EDS identification of NPs with sizes below 20 nm is barely possible with the state-of-the-art instrumentation.

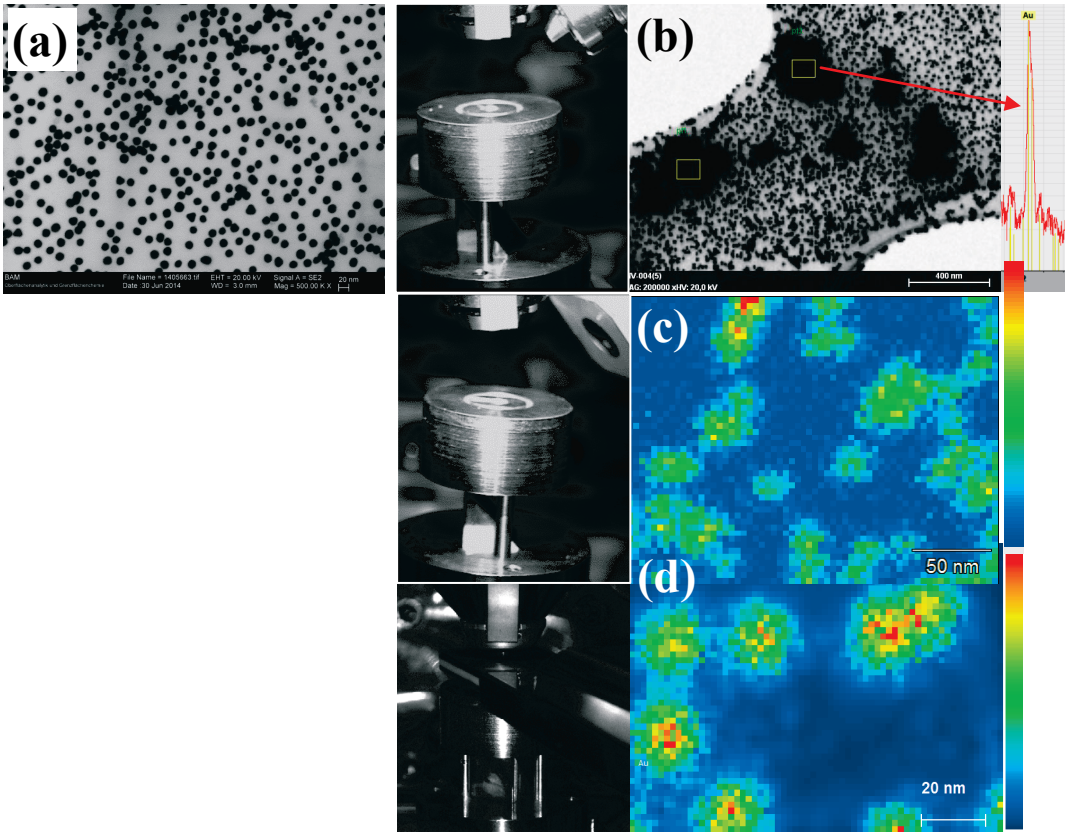

Figure 4. T-SEM/EDS characterisation of 17 nm Au NPs which were prepared on a carbon foil TEM grid. (a) T-SEM micrograph showing the contrast and separation of the individual NPs. (b-d) Chamberscope photos (left) of the various T-SEM/EDS setups and EDS maps (right) of the Au Mα X-ray line. For T-SEM/EDS the screening ring has to be removed (compare to figure 1d). (b) EDS spectrum of Au NP agglomerates acquired with a 10 mm^2 SDD (20 kV, 218 pA). (c) EDS map in false colour display acquired with a 100 mm^2 SDD (20 kV, 441 pA, 64 x 48 pixels, 237 s). (d) EDS map in false colour display acquired with an annular SDD (20 kV, 485 pA, 64 x 48 pixels, 13 s).

The fourth example focusses on the certified reference material (CRM) BAM-L200 [15, 16], a sample which is ideally suited for the determination of the spatial resolution of EDS. The material (GaAs) contains sub-micrometre to -nanometre sized Al doped GaAs stripe structures ($Al_{(0.70)}Ga_{(0.30)}As$) with certified periods and/or widths. The EDS linescan of Ga Lα and Al Kα-lines as acquired with a 10 mm^2 Si(Li) on the cross-sectioned bulk sample of BAM-L200 can be seen in figure 5a. The smallest resolved structure is the "P4" stripes period of 193 nm. Using a 100 mm^2 SDD for a FIB prepared TEM lamella of nominal thickness of 100 nm (figures 5b,c), the "P5" grating

period of 136 nm is clearly resolved, which demonstrates the significant improvement in the spatial EDS resolution. The presence of "W5" stripe of 19.5 nm width is just detected close to the noise level. These studies confirm recent results on the detection of structures in the range of only a few nm in the case of FIB lamellas analysed by large-area SDDs [16]. It should be noted that the finally attained spatial resolution is a function of the geometrical collection efficiency of the EDS detector, of the specimen thickness, but also of the counting statistics. The imaging, nevertheless, at high magnification, even if drift corrected, proceeds mostly within a limited acquisition time. A higher signal-to-noise ratio of the emitted EDS spectra from single NPs can be obtained from high-sensitivity EDS detectors.

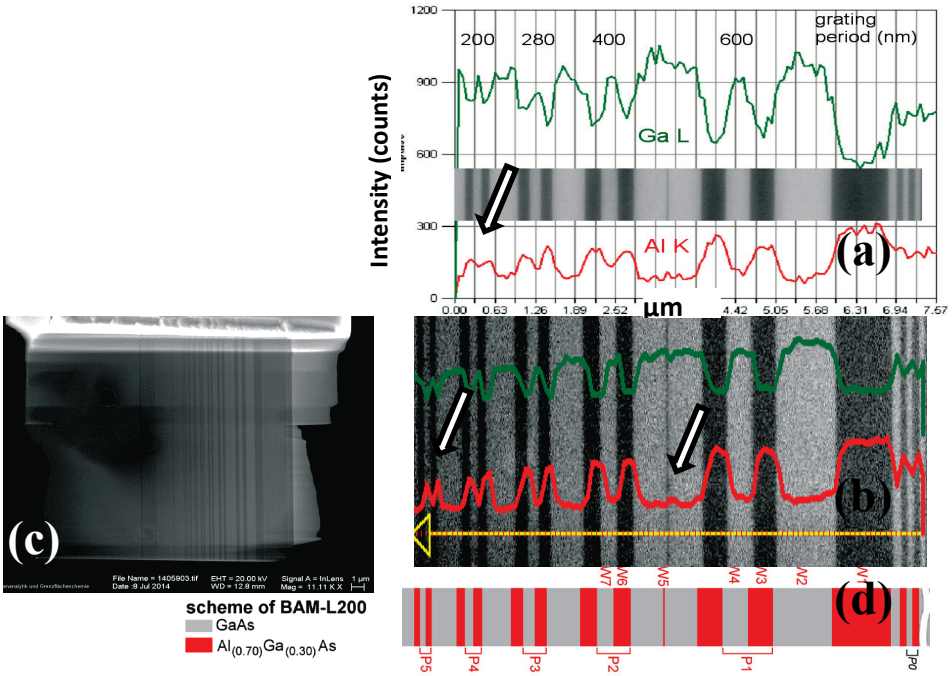

Figure 5. EDS linescans of Ga Lα (green) and Al Kα (red) over corresponding stripe structures from certified reference material BAM-L200. Different spatial resolutions correspond to (a) bulk sample and (b) TEM lamella. The arrows indicate the smallest structures resolved: P4 grating period (193 nm) in case (a), P5 grating period (136 nm), and, close to the noise limit, the stripe W5 (19.5 nm), respectively, in (b). (c) Overview micrograph of the TEM lamella as prepared by FIB of the BAM-L200 bulk sample. Variable thickness is suggested by a hole visible on the upper left side; (d) sketch with corresponding certified structures as denoted in the BAM-L200 certificate [15].

The last application example demonstrates the possibility of automated particle classification using feature analysis with stage control. The motorized sample stage of modern SEMs enables steering with a precision of several micrometres. The automatic acquisition of a large number of micrographs allows analysing a statistically relevant number of NPs. Commercially available software packages which are based on combined SEM and EDS analysis can be applied to the classification of NPs. The case study will present adapted T-SEM/EDS instrumental conditions to classify particles after appropriate deposition (clean and well dispersed) on electron-transparent supporting foils. An analytical workflow consisting of three steps was devised to classify two main classes of SiO_2 particles

of different "consistencies" visible at best in the T-SEM mode (figure 6a): "bulk" (the darker ones) and "hollow" (the brighter ones).

Figure 7 illustrates the sequence of steps to be applied for measurement comprising of (i) identification of the particles according to their corresponding contrast in the transmission (T-SEM) micrographs, (ii) subsequent EDS measurement on the identified particles only, and (iii) chemical classification based on the EDS results.

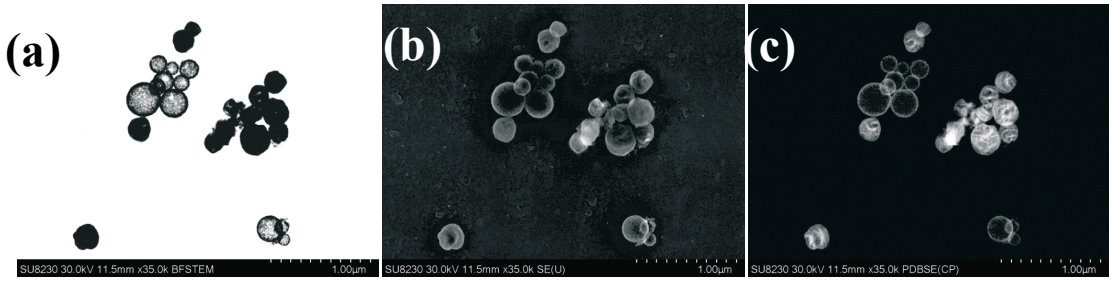

Figure 6. SEM micrographs showing two classes ("bulk" and "hollow") of SiO_2 particles as obtained (a) in the bright-field T-SEM mode, (b) with the conventional SE (upper) detector, and (c) with a BSE detector.

1. Features of interest are first detected in T-SEM micrographs using image processing (figure 7c). Instrumental parameters such as magnification, number of pixels, scan speed were optimized (see Table 1).

Table 1. Parameters of image analysis for the detection of particles in T-SEM micrographs.

Parameter	Setting
Magnification	10,000 x
Image resolution	3,000 x 2,250 pixel
Pixel size	4 nm
Grey level threshold	0 - 145
Circularity	≤ 1.37

It is important to set a grey level threshold within the T-SEM micrograph to accurately distinguish particles from the substrate according to their corresponding contrast. The "hollow" particles (consisting only of an ultra-thin shell) have almost the same T-SEM contrast in the centre as the supporting foil; the particle boundaries are somewhat darker. Therefore, the post-binary filter "Fill Hole" was used in order to improve the detection of particles. The morphological parameter:

$$\text{Circularity} = \frac{\pi \,\text{maxFeret}^2}{4\,\text{Area}}, \tag{1}$$

a dimensionless measure near 1 for round particles and above 1 for irregular particles, was applied in order to accept single NPs and reject agglomerates. By doing so, we assume that all the separated particles have same size distribution and same chemistry as those agglomerated. Extraction of information from agglomerated (or aggregated) particles is physically very little possible (at the outer boundaries).

2. Subsequently, EDS spectra on the identified single particles are automatically acquired. The acquisition time is the decisive parameter, so that sufficient signal-to-noise ratios can be attained in a short time. Due to the high solid angle of the annular SDD, a current of 216 pA and accelerating voltage of 5 kV resulted in an input count rate of 4 - 27 kcps, so that an acquisition time of just 2 seconds per spectrum was sufficient for chemical classification. This is significantly shorter than the spectrum acquisition time of 120 s with a 10 mm^2 SDD where an accelerating voltage of 10 kV and current of 115 pA led to an input count rate of just 50 - 250 cps.
3. The last step comprises reviewing the acquired EDS spectra to setup classes by evaluating the Si K / C K line net intensity ratio and the Si-K net intensities. "Bulk" particles were classified with a Si/C ratio ≥ 1.4 and Si net intensities > 6,000 counts, "hollow" particles correspond to a Si/C ratio ≤ 1.14 and Si net intensities < 4500 counts (figure 7d).

The method was developed at one mesh of the TEM grid (figure 7a) which consists of 35 T-SEM micrographs (figure 7b). This was then applied to four meshes using stage control (figure 7a and Table 2). The whole feature analysis run took 3h24 min, the most of the time was spent on T-SEM micrograph recording. Spectrum acquisition took no more than 14 min altogether.

To verify whether the net intensities are dependent on the "bulk"/"hollow" structure or the particle size, the evaluated data are shown in figure 8. Figure 8a shows that the net intensity ratio of Si K-lines to O K-lines of all classified particles are not dependent upon grey level. This indicates that the chemical composition of the SiO_2 particles does not vary between "bulk" and "hollow" particles. Similarly, the diagram of the Si K to O K net intensity ratio versus particle average diameter (figure 8b) indicates that the particle size has no relationship to the main elemental composition of the SiO_2 particles. In addition, figure 8b points out that most "bulk" particles are larger than the "hollow" ones.

Table 2. Classified particles using automated feature analysis.

Class	Number
Bulk	128
Hollow	104
Unclassified	185
Total	417

It can be summarized that without need of accurate elemental quantification, the qualitative evaluation of the chemical composition of SiO_2 particles of different inner morphologies ("consistencies") by means of the T-SEM/EDS automated analysis is possible. The range of applications of T-SEM/EDS is extended to further examples of complex NP shape and compositions such as core-shell structures. One particular application is wear particles (at both nano- and microscale) in synthetic (additivated as well as non-additivated) oil after lubricated tribological testing [17].

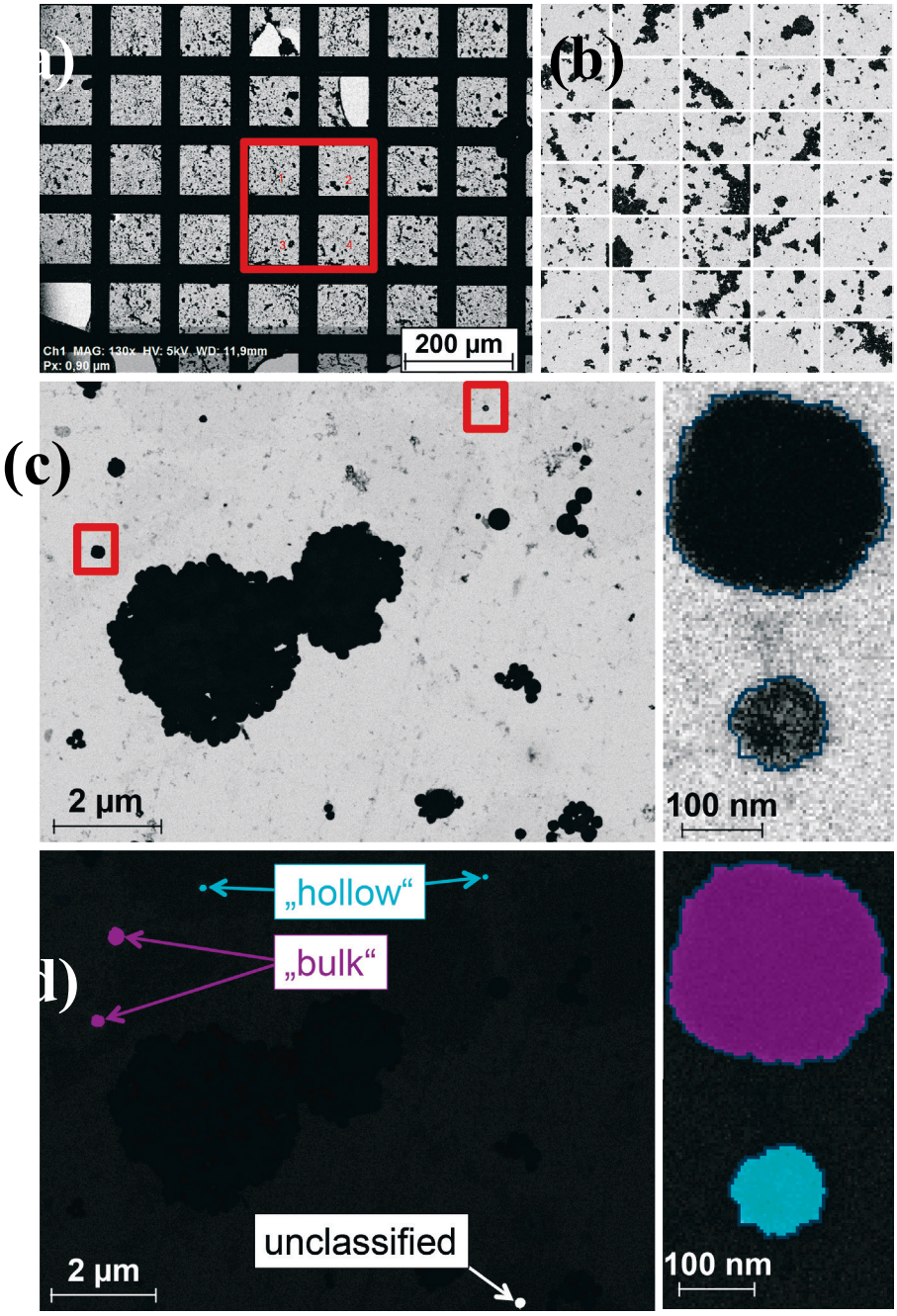

Figure 7. Classification of particles using automated feature analysis. (a) T-SEM micrograph providing an overview of the analysed area (red rectangle) with SiO_2 NPs which were deposited on a TEM grid (150 µm mesh copper) with carbon thin foil. (b) Mosaic of one analysed mesh of the TEM grid consisting of 35 fields. (c) T-SEM micrograph (left) of one analysed field. Red rectangles mark two particles (right) which were detected by image analysis using a corresponding greyscale threshold and the post-binary filter "Fill hole". (d) Feature analysis result overlain with T-SEM micrograph showing classified bulk (violet) and hollow (turquoise) particles which were classified by the Si K / C K line net intensity ratio and the Si-K net intensities.

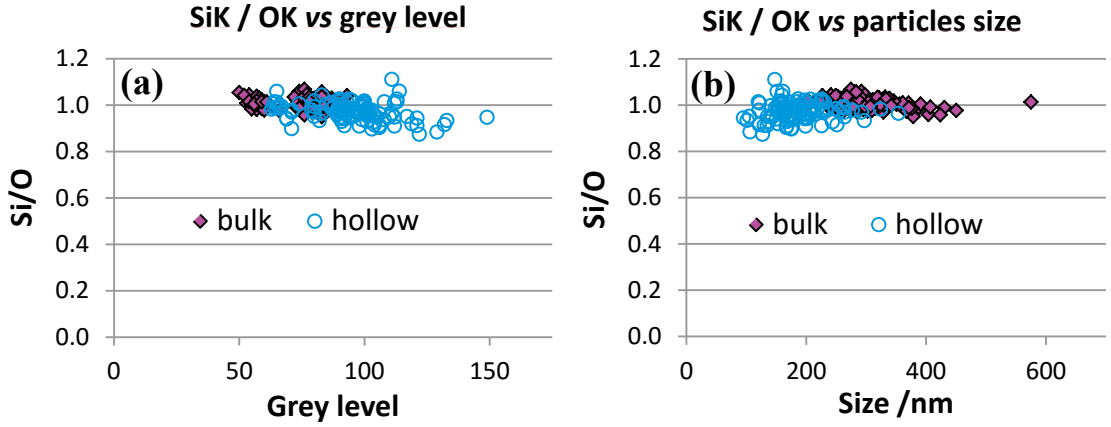

Figure 8. Representation of the chemical composition of 232 classified SiO_2 particles: (a) Si K / O K intensity ratio in dependence on the grey level, and (b) Si K / O K intensity ratio in dependence on the particles size as measured automatically in the T-SEM images.

4. Conclusions

This study provides a detailed overview of the instrumental and methodical possibilities offered by modern SEM/EDS systems for the advanced characterisation of NPs. It demonstrates that high-resolution SEM imaging provides information on the morphology, size, shape and the inner structure of NPs. In addition, advanced EDS spectrum imaging has become possible which adds essential chemical characterisation of nanoparticulate materials.

Two methodical/instrumental approaches enable this analytical undertaking: (i) T-SEM: Preparation of the nanoparticulate material onto electron-transparent foils and operation of the SEM in transmission mode, and (ii) EDS: Use of a high-sensitivity, high solid angle SDD.

A specific application was developed by combining both methods which allows the automated classification of NPs. The advanced software options included within modern analytical systems combine both methods. The image analysis of high contrast T-SEM micrographs provides numerous morphological parameters. The chemical information obtained from EDS spectra are taken only from the identified NPs. This significantly reduces acquisition time as the number of analysed particles is limited to only those that are of potential interest. The spatial resolution is furthermore addressed by T-SEM/EDS for the particular experimental conditions that were evaluated by means of a suitable certified reference material.

The potential of the methodical approach presented in this case study on relatively simple materials can serve as a basis for its application to nanoparticulate commercial products of more complex morphologies and chemical composition. Challenging studies taking into account material characteristics have to be carried out systematically.

Acknowledgements

The research leading to these results has received funding from the European Union's Seventh Framework Programme (FP7/2007-2013) under grant agreement n° 263147 (NanoValid), n° 604347 (NanoDefine) and n° 604577 (SETNanoMetro). Thanks are due to Charles Motzkus (LNE, Paris, France) for the preparation of the aerosol SiO_2 bimodale NPs from figure 2, to W. Österle and R. Hesse for the preparation of the FIB lamella of the BAM-L200 sample (figure 5) and Bruker Nano GmbH (Berlin, Germany) for the measurements with the annular SDD. John Spratt (NHM) is gratefully acknowledged for suggestions improving the manuscript.

References

[1] Buhr E, Senftleben N, Klein T, Bergmann D, Gnieser D, Frase C G and Bosse H 2009 Characterization of nanoparticles by scanning electron microscopy in transmission mode. *Meas. Sci. Technol.* **20** 084025

[2] Klein T, Buhr E, Johnsen K-P and Frase C G 2011 Traceable measurement of nanoparticles size using a scanning electron microscope in transmission mode (TSEM). *Meas. Sci. Technol.* **22** 094002

[3] Motzkus C, Macé T, Gaie-Levrel F, Ducourtieux S, Delvallee A, Dirscherl K, Hodoroaba V-D, Popov I, Popov O, Kuselman I, Takahata K, Ehara K, Ausset P, Maillé M, Michielsen N, Bondiguel S, Gensdarmes F, Morawska L, Johnson G R, Faghihi E M, Kim C S, Kim Y H, Chu M C, Guardado J A, Salas A, Capannelli G, Costa C, Bostrom T, Jäamting Å K, Lawn M A, Adlem L and Vaslin-Reimann S 2013 Size characterization of airborne SiO_2 nanoparticles with on-line and off-line measurement techniques: an interlaboratory comparison study. *J. Nanoparticle Res.* **15**, 1919

[4] Hodoroaba V-D, Motzkus C, Macé T and Vaslin-Reimann S 2014 Performance of high-resolution SEM/EDX systems equipped with transmission mode (TSEM) for imaging and measurement of size and size distribution of spherical nanoparticles. *Microsc. Microanal.* **20** 602-612

[5] Hodoroaba V-D, Akcakayiran D, Grigoriev D O and Shchukin D G 2014 Characterization of micro- and nanocapsules for self-healing anti-corrosion coatings by high resolution SEM with coupled transmission mode and EDX. *Analyst* **139** 2004-2010

[6] Rades S, Wirth T and Unger W E S 2014 Investigation of silica nanoparticles by Auger electron spectroscopy (AES). *Surf. Interface Anal.* **46** 1096-9918

[7] Rades S, Hodoroaba V-D, Salge T, Wirth T, Pilar Lobera M, Hanoi Labrador R, Natte K, Behnke T, Gross T and Unger W E S 2014 High-resolution imaging with SEM/T-SEM, EDX and SAM as a combined methodical approach for morphological and elemental analyses of single engineered nanoparticles. *RSC Adv.* **4** 49577-49587

[8] Crawford B J and Liley C R W 1970 A simple transmission stage using the standard collection system in the scanning electron microscope. *J. Phys. E: Sci. Instrum.* **3** 461-462

[9] Woolf R J, Joy D C and Tansley D W 1972 A transmission stage for the scanning electron microscope. *J. Phys. E: Sci. Instrum.* **5** 230-233

[10] Reimer L, Gentsch P and Hagemann P 1975 Anwendung eines Rasterzusatzes zu einem Rasterelektronenmikroskop. I Grundlagen und Abbildung amorpher Objekte. *Optik* **43** 431-452

[11] Hodoroaba V-D, Rades S and Unger W E S 2014 Inspection of morphology and elemental imaging of single nanoparticles by high resolution SEM/EDX in transmission mode. *Surf. Interface Anal.* **46** 945-948

[12] Vermeulen J P and Jaksch H 2005 A novel STEM detector system. *Imaging and Microscopy* **1** 22-23

[13] Golla U and Schindler B 2004 US Patent 6 815 678 B2

[14] Rasband W S 1997–2012. *Image J*, Bethesda, Maryland, USA: US National Institute of Health. Available at http://rsb.info.nih.gov/ij/ (accessed 22-05-2015)

[15] www.webshop.bam.de, Reference Materials, Layered materials, BAM-L200 (accessed 05-06-2015)

[16] Senoner M, Maassdorf A, Rooch H, Österle W, Malcher M, Schmidt M, Kollmer F, Paul D, Hodoroaba V-D, Rades S and Unger W E S 2015 Lateral resolution of nanoscaled images delivered by surface-analytical instruments: application of the BAM-L200 certified reference material and related ISO standards. *Anal. Bioanal. Chem.* **407** 3211-3217

[17] Wäsche R, Hartelt M and Hodoroaba V-D 2015 Analysis of nanoscale wear particles from lubricated steel-steel contacts. *Tribol. Lett.* **58** 49